

# Model Predictive Controller for Path Following Applications

Ádám Domina<sup>1a</sup>, Viktor Tihanyi<sup>1</sup>

<sup>1</sup> *Department of Automotive Technologies, Faculty of Transportation Engineering and Vehicle Engineering, Budapest University of Technology and Economics*

<sup>a</sup> *Corresponding author: domina.adam@kjk.bme.hu*

## Abstract

*In this article, a model predictive controller (MPC) for automated vehicle path following is presented. The MPC calculates the optimal steering command based on the prediction of the future states of the vehicle and the reference given for the controller. The aim is to minimize the difference between the predicted and the reference states, which is ensured by the optimal control input. The MPC control technique applies a vehicle model for state prediction. In this paper, a bicycle model is used for state prediction, which model is updated at every time step formalizing an LPV-MPC structure. The controller aims to minimize the lateral and angular deviation of the vehicle from a fixed path. A reference path is built, on which the controller is tested, showing a good performance.*

**Keywords:** *automated vehicle, MPC, vehicle model*

## 1 Introduction

The advanced driver-assistance systems, collision avoidance systems, and the different automated vehicle functions are getting more popular in recent years. The improvement of automated vehicles allows the potential to reduce pollutant emissions, the number of accidents, improve road safety and ensure safer transport. In the hierarchical software structure of an automated vehicle, the motion control layer is responsible for the lateral and longitudinal motion control of the vehicle. In this article, the authors mainly focus on lateral control, which is realized by the steering system in an automated vehicle. The longitudinal dynamics is controlled separately by a PI cruise controller.

In this paper, a MPC is applied for following a path from the numerous existing path following solutions presented in [1], [2], and [3]. The authors decided to apply the MPC technique because this controller includes both features required for accurate path tracking, are 1) the dynamics of the vehicle is applied for the calculation of the necessary steering angle as a control input and 2) the controller has information about the reference path ahead of the vehicle. Furthermore, MPC can handle constraints well, in this case, the constraints are applied as limits of the actuator intervention, as maximal steering angle values.

The controller is tested on a predefined path, using different vehicle speeds, the tests proved the practicality of the proposed controller, the performance is good, the vehicle can follow the path with small lateral and angle errors. The organization of this paper is as follows. Section II describes the applied vehicle models, Section III presents the MPC structure, Section IV considers the results, and finally, the results and concluding remarks are summarized in Section V.

## 2 Vehicle modeling

Two different vehicle models were applied in this article one for testing the performance of the controller and another for state prediction by the MPC.

### 2.1 Vehicle model for testing the controller

A three-state dynamic bicycle model [4] is used for testing the controller in a simulation environment. The model considers solely the planar dynamics of the vehicle, the pitching and the rolling dynamics are neglected, because these do not have a significant effect on our investigation. The states of the vehicle model are the yaw-

rate of the vehicle, the longitudinal velocity, and the sideslip angle at the center of gravity (C.G.). The derivative of the states is calculated by (1), (2), and (3).

$$\dot{r} = \frac{aF_{yF} - bF_{yR}}{I_z} \quad (1)$$

$$\dot{V}_x = \frac{F_{xR} - F_{yF} \sin(\delta)}{m} + rV_x \beta \quad (2)$$

$$\dot{\beta} = \frac{F_{yF} + F_{yR}}{mV_x} - r \quad (3)$$

where  $r$  is the yaw-rate,  $a$  and  $b$  are the distance from C.G. to front and rear axle, respectively,  $I_z$  is the moment of inertia around axis  $z$ ,  $F_{yF}$  and  $F_{yR}$  are the lateral forces at the front and at the rear wheels, respectively,  $F_{xR}$  is the traction force at the rear wheel,  $\delta$  is the steering angle,  $m$  is the mass of the vehicle,  $V_x$  and  $V_y$  are the longitudinal and the lateral velocity of the vehicle in the ego frame, respectively, and  $\beta$  is the sideslip angle of the vehicle. The bicycle model and the notations are shown in Fig. 1, where  $\alpha_F$  and  $\alpha_R$  are the sideslip angles at the front and the rear axles, respectively.

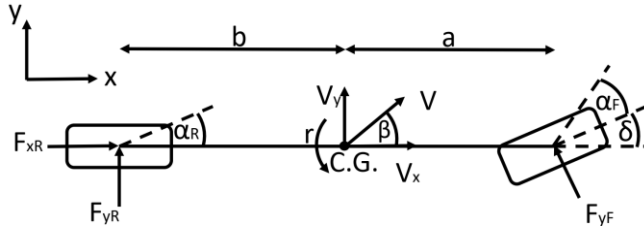


Fig. 1 Three-state bicycle model

The lateral dynamics of the tires is modeled by a Brush tire model (4), (5) which is enhanced with a  $\zeta$  derating factor (6) at the rear wheels for considering the reduction of the maximal transferable lateral force. At the front wheel, the value of  $\zeta$  is fixed as  $\zeta=1$  since there is solely lateral force applied, assuming a rear-wheel-drive vehicle.

$$F_y = \begin{cases} -C_\alpha \tan(\alpha) + \frac{C_\alpha^2}{3\zeta\mu F_z} |\tan(\alpha)| \tan(\alpha) - \frac{C_\alpha^3}{27\zeta^2\mu^2 F_z^2} \tan^3(\alpha), & |\alpha| \leq \alpha_{sl} \\ -\zeta\mu F_z \text{sgn}(\alpha), & |\alpha| > \alpha_{sl} \end{cases} \quad (4)$$

$$\alpha_{sl} = \frac{3\zeta\mu F_z}{C_\alpha} \quad (5)$$

$$\zeta = \sqrt{\frac{(\mu_R F_{zR})^2 - F_x^2}{\mu_R F_{zR}}} \quad (6)$$

where  $C_\alpha$  is the cornering stiffness of the tires,  $\alpha$  is the sideslip angle,  $\mu$  is the friction coefficient,  $F_z$  is the normal load on the wheels. The sideslip angles are calculated by (7) and (8).

$$\alpha_F = \arctan \frac{V_y + ar}{V_x} - \delta \approx \arctan \left( \beta + \frac{a}{V_x} r \right) - \delta \quad (7)$$

$$\alpha_R = \arctan \frac{V_y - br}{V_x} \approx \arctan \left( \beta - \frac{b}{V_x} r \right) \quad (8)$$

## 2.2 Vehicle model for state prediction

While the MPC is a discrete-time controller structure, a continuous-time state-space representation of the vehicle is formalized and transformed to a discrete-time model. The state-space representation of the vehicle is calculated at every time step based on the current state of the vehicle. A lateral dynamic bicycle model (9) is applied for state prediction which is presented in [5], the state vector is  $x = [e_{lat} \ \dot{e}_{lat} \ e_{ang} \ \dot{e}_{ang}]^T$ , where  $e_{lat}$  is the lateral error,  $e_{ang}$  is the angle error, the derivative of the vehicle state vector is calculated as  $\dot{x} = Ax + Bu$ .

$$A = \begin{bmatrix} 0 & 1 & 0 & 0 \\ 0 & -\frac{2C_{\alpha f} + 2C_{\alpha r}}{mV_x} & \frac{2C_{\alpha f} + 2C_{\alpha r}}{m} & -\frac{2C_{\alpha f}l_f + 2C_{\alpha r}l_r}{mV_x} \\ 0 & 0 & 0 & 1 \\ 0 & -\frac{2C_{\alpha f}l_f - 2C_{\alpha r}l_r}{I_zV_x} & \frac{2C_{\alpha f}l_f - 2C_{\alpha r}l_r}{I_z} & -\frac{2C_{\alpha f}l_f^2 - 2C_{\alpha r}l_r^2}{I_zV_x} \end{bmatrix}, \quad B = \begin{bmatrix} 0 \\ \frac{2C_{\alpha f}}{m} \\ 0 \\ \frac{2C_{\alpha f}l_f}{I_z} \end{bmatrix} \quad (9)$$

The vehicle model applies a linear tire model, where the lateral force is linearly proportional with the sideslip angle for the entire sideslip domain, which approximation is considered correct if the tires operate on the linear region of the tire characteristics which is shown in Fig. 2.

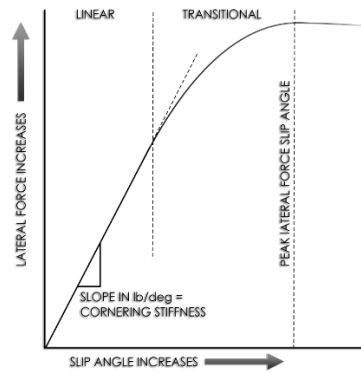


**Fig. 2** Characteristics of a tire

The lateral and angular errors are interpreted at the closest point of the reference path.

### 3 MPC structure

The controller aims to drive the vehicle along the path while the lateral and angular errors converge to zero and stay at this value. The basic advantage of MPC is the continuous online optimization based on a built-in system model. The controller computes the series of the optimal control inputs in every time step as a row vector for a fixed horizon which is the control horizon ( $N_c$ ) and applies only the first element of the vector on the controlled system. The control objective is defined by a cost function that needs to be minimized by the optimization. In this case, the cost function is (10)

$$J = (R_s - Y)^T (R_s - Y) + \Delta U^T \bar{R} \Delta U \quad (10)$$

where  $R_s$  vector contains the reference, which is a zero vector in this case, since the reference lateral and angle errors is zero,  $Y$  is the system output vector and  $U$  is the control input. The reference is defined as (11), where  $r(k_i)$  contains the zero values as references.

$$R_s^T = \overbrace{[1 \ 1 \ \dots \ 1]}^{N_p} r(k_i) \quad (11)$$

$$Y = Fx(k_i) + \phi \Delta U \quad (12)$$

$$F = \begin{bmatrix} CA \\ CA^2 \\ CA^3 \\ \vdots \\ CA^{N_p} \end{bmatrix}; \phi = \begin{bmatrix} CB & 0 & 0 & \dots & 0 \\ CAB & CB & 0 & \dots & 0 \\ CA^2B & CAB & CB & \dots & 0 \\ \vdots & \vdots & \vdots & \ddots & \vdots \\ CA^{N_p-1}B & CA^{N_p-2}B & CA^{N_p-3}B & \dots & CA^{N_p-N_c}B \end{bmatrix} \quad (13)$$

where  $F$  and  $\phi$  are used for predicting the states for the prediction horizon. In this paper, the control horizon and the prediction horizon are treated as equal values as  $N_p = N_c$ . The value of  $J$  is minimal when the first derivative of  $J$  is equal to zero. The optimal solution for the control signal  $\Delta U$  is

$$\Delta U = (\phi^T \phi + \bar{R})^{-1} \phi^T (R_s - Fx(k_i)) \quad (14)$$

In (14)  $R$  is reflected in the size of  $\Delta U$  when the objective function  $J$  is made to be as small as possible.  $R$  is a diagonal matrix

$$\bar{R} = r_\omega I_{N_c \times N_c} \quad (r_\omega \geq 0) \quad (15)$$

where  $r_\omega$  is used as a tuning parameter. In the case that  $r_\omega=0$  represents the situation where we would not want to pay any attention to how large the  $\Delta U$  might be and the goal would be solely to make the errors as small as possible. In the case when  $r_\omega$  is large the cost function describes a situation where would carefully consider how large the  $\Delta U$  might be and reduce the error.

## 4 Results

A reference path is built for testing the controller, the tests are conducted at different vehicle velocities. The path is shown in Fig. 3, while the results are presented in Fig. 4 and Fig. 5 for the 40 km/h and the 50 km/h cases, respectively.

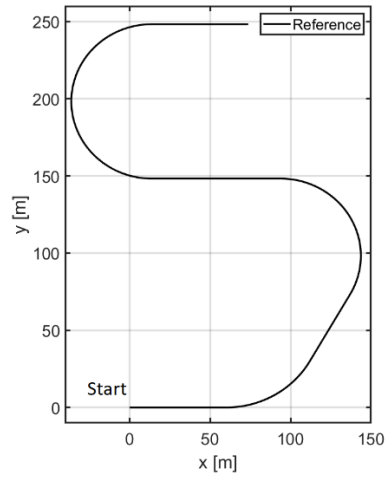


**Fig. 3** The reference path

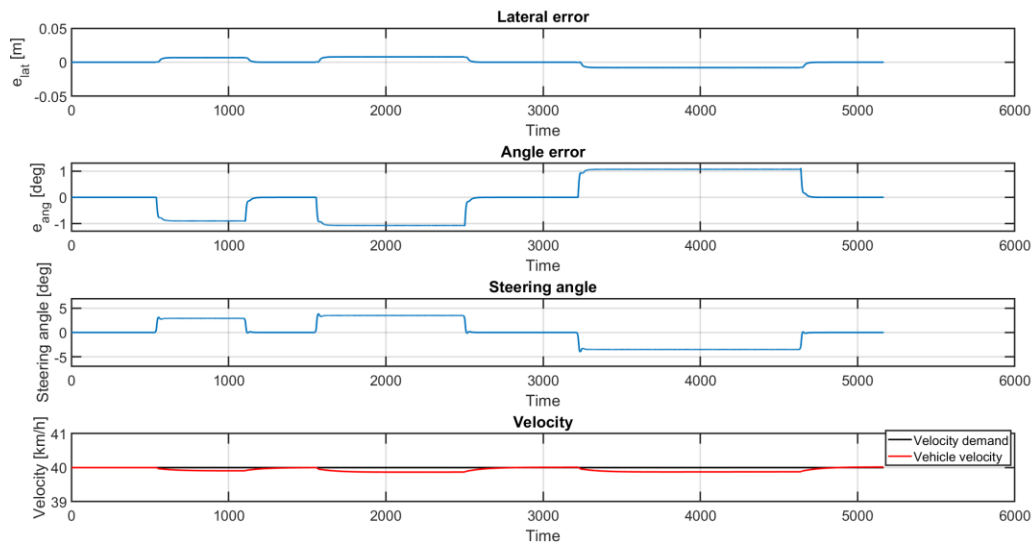


**Fig. 4** The simulation results at 40 km/h

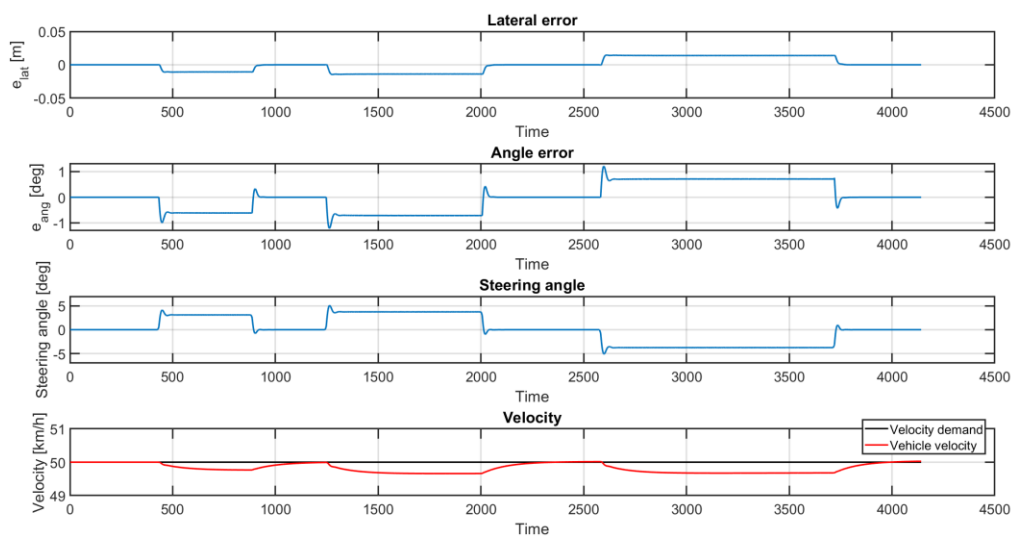


**Fig. 5** The simulation results at 50 km/h

As shown by the steering angle in Fig. 5, the controller tends to become unstable at 50 km/h, due to the higher sideslip angles reached at the corners. As stated before, the state prediction is based on a linearized tire model, which is modeling the tire behavior correctly solely on the linear region. Beyond the linear region, the state prediction becomes incorrect which is responsible for the limited application of the controller. However, at moderate vehicle velocity, the controller shows an accurate and stable path following performance.

## 5 Conclusion

In this paper, a MPC for automated vehicle path following application is proposed. The controller proved to be stable until 50 km/h vehicle velocity, where the predicted and the real states are started to deviate from each other due to the nonlinearities of the tires. Thus, the proposed controller is applicable until the tires are operating on the linear region.

Possible further research direction is the inclusion of the tire nonlinearities into the state prediction, e.g. apply a LTV-MPC structure, or nonlinear MPC methods, the disadvantage of which is the higher computational requirement.

## Acknowledgement

The research reported in this paper and carried out at the Budapest University of Technology and Economics has been supported by the National Research Development and Innovation Fund (TKP2020 National Challenges Subprogram, Grant No. BME-NC) based on the charter of bolster issued by the National Research Development and Innovation Office under the auspices of the Ministry for Innovation and Technology.

## References

- [1] Z. Lu, B. Shyrokau, B. Boulkroune, S. van Aalst and R. Happee, "Performance benchmark of state-of-the-art lateral path-following controllers," 2018 IEEE 15th International Workshop on Advanced Motion Control (AMC), 2018, pp. 541-546, doi: 10.1109/AMC.2019.8371151.
- [2] Viana, I. B., Kanchwala, H., Ahiska, K., and Aouf, N. (February 4, 2021). "A Comparison of Trajectory Planning and Control Frameworks for Cooperative Autonomous Driving." ASME. J. Dyn. Sys., Meas., Control. July 2021; 143(7): 071002. <https://doi.org/10.1115/1.4049554>
- [3] Í. B. Viana, H. Kanchwala and N. Aouf, "Cooperative Trajectory Planning for Autonomous Driving Using Nonlinear Model Predictive Control," 2019 IEEE International Conference on Connected Vehicles and Expo (ICCVE), 2019, pp. 1-6, doi: 10.1109/ICCVE45908.2019.8965227
- [4] R. Hindiyeh, "Dynamics and control of drifting in automobiles," PhD dissertation, Stanford University, 2013.
- [5] R. Rajamani, "Vehicle dynamics and control," in Mechanical Engineering Series, 2nd ed. Springer, Boston, MA, 2012.